RESEARCH ARTICLE

Dielectric and Ferroelectric Properties of $Ba_{0.85}Ca_{0.15}Ti_{0.9}Zr_{0.1}O_3$–$Sr_{0.7}Bi_{0.2}TiO_3$ Solid Solution

Kainat Shah[1,*] **and Asif Ali**[1]

[1] Department of Physics, Abdul Wali Khan University Mardan, Mardan 23200, KP, Pakistan

Abstract

In this work, $(1-x)Ba_{0.85}Ca_{0.15}Ti_{0.9}Zr_{0.1}O_3 - xSr_{0.7}Bi_{0.2}TiO_3$ **(BCZT–SBT) ceramics with** $x = 0$ **and** $x = 0.025$ **were prepared through the conventional solid-state route. The samples were calcined at** $1200\,^{\circ}C$ **for** $6\,h$**, then re-milled, pressed into pellets, and sintered at** $1325\,^{\circ}C$ **for** $6\,h$**. XRD patterns indicate the formation of a cubic perovskite structure. A small decrease in lattice parameter is observed upon introducing SBT (**a **decreases from** $4.0176\,Å$ **to** $4.0149\,Å$**), accompanied by a slight reduction in unit-cell volume (**$64.85\,Å^3$ **to** $64.72\,Å^3$**).** ε_r **increases strongly with** $x = 0.025$**: at** $1\,MHz$**,** ε_r **rises from 1057 (**$x = 0$**) to 2175 (**$x = 0.025$**), while** $\tan\delta$ **remains low (0.034–0.037). Ferroelectric measurements at** $30\,kV/cm$ **show an increase in maximum polarization from** $11.06\,\mu C/cm^2$ **(**$x = 0$**) to** $23.5\,\mu C/cm^2$ **(**$x = 0.025$**), with the coercive field decreasing from** $6.9\,kV/cm$ **to** $5.1\,kV/cm$**.**

Keywords: BCZT, SBT, dielectric properties, ferroelectric properties.

1 Introduction

Lead-based ferroelectric ceramics, particularly $Pb(Zr,Ti)O_3$ (PZT), have been used for decades because they combine high permittivity with strong polarization response, enabling sensors, transducers, and capacitor technologies [1, 2]. Their toxicity, however, motivates the continued development of lead-free compositions that can provide comparable functional response without regulatory and environmental complications [3, 4]. Among lead-free perovskites, Ba-based solid solutions in the $(Ba,Ca)(Ti,Zr)O_3$ family have attracted attention because their electrical properties can be tuned through composition and processing, including the possibility of enhanced response near phase boundaries [5, 6]. Reported studies also emphasize that calcination/sintering conditions, grain size, and densification substantially influence dielectric loss and permittivity trends, making processing control a key part of the materials design problem [7–11]. In parallel, Sr–Bi–Ti–O based relaxor-type ceramics have been studied due to their diffuse dielectric features, often linked to A-site disorder/vacancies and off-centering behavior [12–14]. These materials motivate compositional strategies in which a relaxor-like component is combined with a ferroelectric perovskite matrix to modify polarization dynamics and dielectric response.

Submitted: 24 February 2026
Accepted: 26 March 2026
Published: 28 March 2026

Vol. 2, **No.** 1, 2026.
10.62762/JAEM.2026.678918

***Corresponding author:**
✉ Kainat Shah
kainat.lfmd@gmail.com

Citation
Shah, K., & Ali, A. (2026). Dielectric and Ferroelectric Properties of $Ba_{0.85}Ca_{0.15}Ti_{0.9}Zr_{0.1}O_3$–$Sr_{0.7}Bi_{0.2}TiO_3$ Solid Solution. *Journal of Advanced Electronic Materials*, 2(1), 20–24.

The present study focuses on only two compositions: BCZT (x = 0) and a lightly modified BCZT–SBT solid solution (x = 0.025), prepared under the same processing schedule. Restricting the manuscript to these two samples allows the structural and electrical comparisons to be stated cleanly and avoids over-interpreting non-monotonic trends that appear when many compositions are combined without consistent densification and microstructural control.

2 Experimental Methods

Stoichiometric amounts of high purity $BaCO_3$ (99.9%), $CaCO_3$ (99.9%), Bi_2O_3 (99.9%), $SrCO_3$ (99.9%), TiO_2 (99%) powders, retrieved from Sigma Aldrich and ZrO_2 (99%) of UNI-Chem were dried to remove moisture prior to weighing. For $x = 0$ and $x = 0.025$, powders were mixed and milled to reduce particle size, break agglomerates, and improve compositional homogeneity. In this work, milling was carried out using an agate mortar and pestle for 2 h, with acetone used as a solvent; the milled slurry was dried at 150 °C for 30 min.

Calcination was used to promote carbonate decomposition, remove volatile species (e.g., CO_2), and drive the solid-state reaction toward perovskite phase formation. The mixed powders were calcined at 1200 °C for 6 h in a muffle furnace, using a heating rate of 5 °C/ min, then re-milled to obtain a finer powder. Pellets (10 mm diameter) were pressed using a hydraulic press at ∼0.5 ton to a thickness of a few millimeters. Sintering was performed to densify the pellets by diffusion-driven mass transport and pore elimination. For the two compositions retained in this manuscript, pellets were sintered at 1325 °C for 6 h.

Phase formation was examined using a Philips X-ray diffractometer (Cu-Kα, $\lambda = 1.54$ Å), scanned from $2\theta = 20°$ to $80°$ with a step size of $0.02°$. The lattice parameters were calculated using the least square method, through WINXPOW package. Dielectric permittivity (ε_r) and dielectric loss ($\tan\delta$) were measured using an LCR meter as a function of frequency from 1 Hz to 1 MHz at room temperature. Polarization-electric field (P-E) hysteresis loops were recorded at room temperature using a PolyK ferroelectric analyzer up to an electric field of 30 kV/cm. Maximum polarization (P_{max}), remnant polarization (P_r), and coercive field (E_c) were extracted from the loops.

3 Results and Discussion

Figure 1 shows the XRD patterns for BCZT ($x = 0$) and BCZT–SBT ($x = 0.025$) ceramics. Within the scanned range, the diffraction peaks are consistent with a perovskite phase and do not reveal obvious secondary-phase reflections at the level detectable by laboratory XRD.

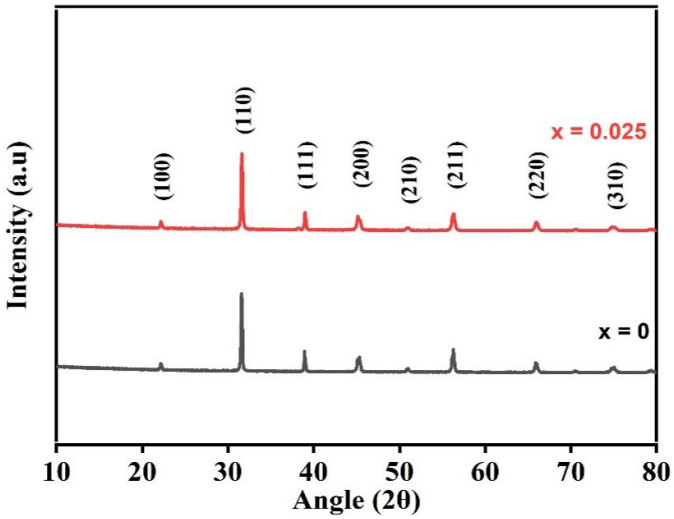

Figure 1. X-ray diffraction patterns of BCZT–SBT ceramics for $x = 0$ and $x = 0.025$ (calcined at 1200 °C/6 h; pellets sintered at 1325 °C/6 h).

This supports a single-phase assignment within the resolution of the measurement. A small shift of peaks toward higher 2θ is consistent with a slight decrease in lattice parameter after introducing $x = 0.025$. This is reflected quantitatively in the refined/estimated lattice parameters: a decrease from 4.0176 Å ($x = 0$) to 4.0149 Å ($x = 0.025$), with unit-cell volume decreasing from 64.85 $Å^3$ to 64.72 $Å^3$. A modest contraction of the average lattice is physically plausible when the average effective ionic size on the relevant crystallographic site(s) decreases [15]. However, the present manuscript does not include Rietveld refinement quality metrics, site-occupancy refinement, or complementary chemical analysis; therefore, the lattice-contraction observation should be interpreted as a robust structural trend, while detailed substitution mechanisms should be stated cautiously. The density of the samples was calculated by using Archimedes' Principle. The samples sintered at 1325 °C/6 h exhibited a relative density of approximately ∼ 90%.

Figure 2 presents ε_r and $\tan\delta$ as a function of frequency (room temperature) for the two retained compositions. Both samples show the common trend of decreasing ε_r with increasing frequency. This behavior is consistent with the frequency-dependent response of polarization

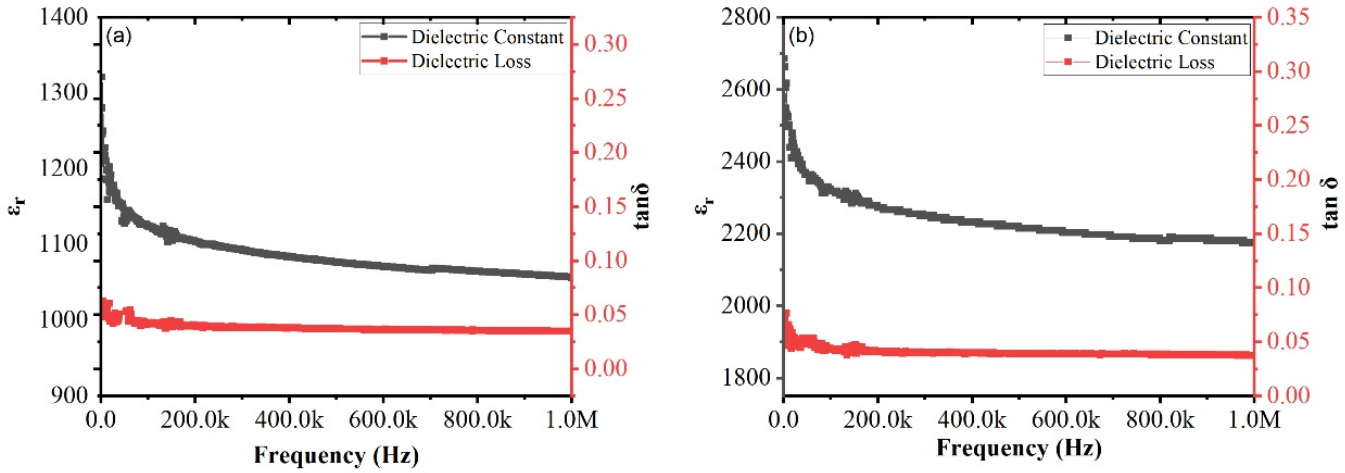

Figure 2. Dielectric permittivity ε_r and dielectric loss $\tan\delta$ versus frequency (room temperature) for BCZT–SBT ceramics with (a) $x = 0$ and (b) $x = 0.025$.

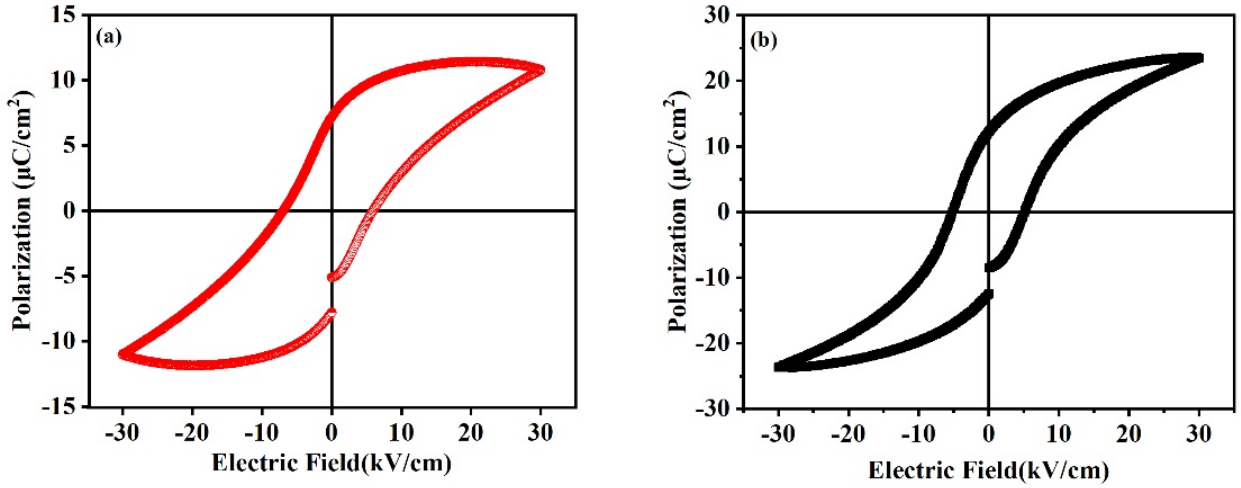

Figure 3. P–E hysteresis loops (room temperature, maximum field $30\,\mathrm{kV/cm}$) for BCZT–SBT ceramics with (a) $x = 0$ and (b) $x = 0.025$.

mechanisms: at low frequency, slower contributions such as space-charge/interfacial polarization and dipolar/domain-wall related processes can respond to the applied field, raising the measured permittivity; as frequency increases, these contributions progressively lag and no longer contribute fully, leaving primarily faster ionic/electronic polarization at the highest frequencies. Quantitatively, at $1\,\mathrm{MHz}$, ε_r increases from 1057 ($x = 0$) to 2175 ($x = 0.025$), while $\tan\delta$ remains low and comparable (0.034 for $x = 0$ and 0.037 for $x = 0.025$). At $1\,\mathrm{kHz}$, ε_r is 1123 ($x = 0$) and 2318 ($x = 0.025$), with $\tan\delta \sim 0.040$ and 0.044, respectively.

Two points follow directly from these data. The $x = 0.025$ composition exhibits a substantially higher ε_r over the full measured frequency window. The increase in ε_r is not accompanied by a disproportionate increase in dielectric loss, since $\tan\delta$ remains in the same low range.

From a materials standpoint, an increased ε_r at fixed frequency can originate from several factors, including changes in intrinsic lattice polarizability, defect chemistry and local structural disorder, and extrinsic contributions such as domain-wall mobility; microstructure (porosity and grain size) can also strongly influence the effective permittivity. The fact that ε_r nevertheless increases suggests that composition-driven polarization effects are strong enough to overcome the porosity penalty under the

present conditions. Pinning down the dominant mechanism would require microstructural and electrical characterization beyond what is currently shown (e.g. grain size distribution, impedance spectroscopy separating grain/grain-boundary response and leakage current assessment).

Ferroelectric hysteresis loops measured at room temperature up to $30\,\mathrm{kV/cm}$ are shown in Figure 3. Both compositions exhibit closed P–E loops, consistent with ferroelectric polarization switching under the applied field. For $x = 0$, the extracted parameters are $P_{\max} = 11.06\,\mu\mathrm{C/cm^2}$, $P_r = 7.3\,\mu\mathrm{C/cm^2}$, and $E_c = 6.9\,\mathrm{kV/cm}$. For $x = 0.025$, $P_{\max}$ increases to $23.5\,\mu\mathrm{C/cm^2}$, P_r increases to $12.7\,\mu\mathrm{C/cm^2}$, and E_c decreases to $5.1\,\mathrm{kV/cm}$. These trends indicate that adding a small fraction of SBT strengthens the polarization response under the same applied field amplitude (higher $P_{\max}$) while reducing the coercive field (lower E_c), implying that polarization reversal occurs at a lower field. In practical terms, a lower E_c can be consistent with easier domain switching and/or modified pinning conditions, but loop shape can also be influenced by conductivity and measurement conditions. The current manuscript does not present leakage current data or field-dependent loop evolution; therefore, interpretations should be limited to what the loops directly show: increased polarization magnitude and a reduced coercive field for $x = 0.025$ at $30\,\mathrm{kV/cm}$.

To contextualize the present results, a comparison with previously reported (1-x)BCZT-xSBT systems is provided. The obtained ε_r values (1057 for $x = 0$ and 2175 for $x = 0.025$) at $1\,\mathrm{MHz}$ are higher than the previously reported values i.e. ~ 750 for $x = 0$ and 0.025 with $\tan\delta \sim 0.1$, as well as the reported $P_r(\sim 14.8\,\mu\mathrm{C/cm^2})$ for $x = 0$ is larger than the obtained value ($7.3\,\mu\mathrm{C/cm^2}$) while $E_c(\sim 5.2\,\mathrm{kV/cm})$ is smaller than the findings ($E_c = 6.9\,\mathrm{kV/cm}$) of this manuscript [16]. However, for $x = 0.1$, the reported P_r is $\sim 5\,\mu\mathrm{C/cm^2}$ which is far lower than the obtained value ($12.7\,\mu\mathrm{C/cm^2}$ for $x = 0.025$) [16]. Whereas another investigation reported $\varepsilon_r(\sim 1200)$ and $\tan\delta(\sim 0.3)$ at $1\,\mathrm{MHz}$ while an extremely small $P_r(\sim 0.86\,\mu\mathrm{C/cm^2})$ for $x = 0.6$ [17].

4 Conclusion

BCZT ($x = 0$) and lightly modified BCZT–SBT ($x = 0.025$) ceramics were fabricated by the solid-state route, calcined at $1200\,^\circ\mathrm{C}$ for $6\,\mathrm{h}$, and sintered at $1325\,^\circ\mathrm{C}$ for $6\,\mathrm{h}$. XRD patterns are consistent with a perovskite phase for both compositions in the scanned range and show a small lattice contraction when $x = 0.025$ is introduced (a decreases from $4.0176\,\text{Å}$ to $4.0149\,\text{Å}$). Despite this, the dielectric response improves strongly with $x = 0.025$: ε_r increases from 1057 to 2175 at $1\,\mathrm{MHz}$ while $\tan\delta$ remains low (0.034–0.037). Ferroelectric measurements at $30\,\mathrm{kV/cm}$ show that $x = 0.025$ yields higher maximum polarization ($23.5\,\mu\mathrm{C/cm^2}$ versus $11.06\,\mu\mathrm{C/cm^2}$) and a lower coercive field ($5.1\,\mathrm{kV/cm}$ versus $6.9\,\mathrm{kV/cm}$). Within the scope of the presented measurements, incorporating a small $Sr_{0.7}Bi_{0.2}TiO_3$ fraction therefore enhances both dielectric permittivity and polarization response in the BCZT matrix.

Data Availability Statement

Data will be made available on request.

Funding

This work was supported without any funding.

Conflicts of Interest

The authors declare no conflicts of interest.

AI Use Statement

The authors declare that generative AI was used solely for language editing and grammatical refinement during the preparation of this manuscript. The AI tool utilized was ChatGPT. The authors carefully reviewed and verified all AI-assisted revisions and take full responsibility for the accuracy, originality, and integrity of the content.

Ethical Approval and Consent to Participate

Not applicable.

References

[1] Zhou, Z., Tang, H., & Sodano, H. A. (2014). Scalable synthesis of morphotropic phase boundary lead zirconium titanate nanowires for energy harvesting. *Advanced Materials (Deerfield Beach, Fla.)*, *26*(45), 7547-7554. [CrossRef]

[2] Koruza, J., Bell, A. J., Frömling, T., Webber, K. G., Wang, K., & Rödel, J. (2018). Requirements for the transfer of lead-free piezoceramics into application. *Journal of Materiomics*, *4*(1), 13-26. [CrossRef]

[3] Panda, P. K., & Sahoo, B. (2015). PZT to lead free piezo ceramics: a review. *Ferroelectrics*, *474*(1), 128-143. [CrossRef]

[4] Rödel, J., Jo, W., Seifert, K. T., Anton, E. M., Granzow, T., & Damjanovic, D. (2009). Perspective on the

development of lead-free piezoceramics. *Journal of the American Ceramic Society, 92*(6), 1153-1177. [CrossRef]

[5] Hanani, Z., Mezzane, D., Amjoud, M. B., Gagou, Y., Hoummada, K., Perrin, C., ... & Rožič, B. (2020). Structural, dielectric, and ferroelectric properties of lead-free BCZT ceramics elaborated by low-temperature hydrothermal processing. *Journal of Materials Science: Materials in Electronics, 31*(13), 10096-10104. [CrossRef]

[6] Liu, W., & Ren, X. (2009). Large piezoelectric effect in Pb-free ceramics. *Physical Review Letters, 103*(25), 257602. [CrossRef]

[7] Wu, J., Xiao, D., Wu, B., Wu, W., Zhu, J., Yang, Z., & Wang, J. (2012). Sintering temperature-induced electrical properties of $(Ba_{0.90}Ca_{0.10})(Ti_{0.85}Zr_{0.15})O_3$ lead-free ceramics. *Materials Research Bulletin, 47*(5), 1281-1284. [CrossRef]

[8] Wang, Z., Wang, J., Chao, X., Wei, L., Yang, B., Wang, D., & Yang, Z. (2016). Synthesis, structure, dielectric, piezoelectric, and energy storage performance of $(Ba_{0.85}Ca_{0.15})(Ti_{0.9}Zr_{0.1})O_3$ ceramics prepared by different methods. *Journal of Materials Science: Materials in Electronics, 27*(5), 5047-5058. [CrossRef]

[9] Praveen, J. P., Karthik, T., James, A. R., Chandrakala, E., Asthana, S., & Das, D. (2015). Effect of poling process on piezoelectric properties of sol–gel derived BZT–BCT ceramics. *Journal of the European Ceramic Society, 35*(6), 1785-1798. [CrossRef]

[10] Rafiq, M. A., Rafiq, M. N., & Saravanan, K. V. (2015). Dielectric and impedance spectroscopic studies of lead-free barium-calcium-zirconium-titanium oxide ceramics. *Ceramics International, 41*(9), 11436-11444. [CrossRef]

[11] Wu, J., Xiao, D., Wu, W., Chen, Q., Zhu, J., Yang, Z., & Wang, J. (2011). Role of room-temperature phase transition in the electrical properties of (Ba, Ca)(Ti, Zr)O_3 ceramics. *Scripta Materialia, 65*(9), 771-774. [CrossRef]

[12] Zhao, P., Tang, B., Si, F., Yang, C., Li, H., & Zhang, S. (2020). Novel Ca doped $Sr_{0.7}Bi_{0.2}TiO_3$ lead-free relaxor ferroelectrics with high energy density and efficiency. *Journal of the European Ceramic Society, 40*(5), 1938-1946. [CrossRef]

[13] Sakurai, M., Kanehara, K., Takeda, H., Tsurumi, T., & Hoshina, T. (2016). Wideband dielectric spectroscopy of (Sr0. 7Bi0. 2) TiO3 ceramics and its microscopic mechanism of polarization. *Journal of the Ceramic Society of Japan, 124*(6), 664-667. [CrossRef]

[14] Zhang, G. F., Cao, M., Hao, H., & Liu, H. (2013). Energy storage characteristics in $Sr_{(1-1.5x)}Bi_xTiO_3$ ceramics. *Ferroelectrics, 447*(1), 86-94. [CrossRef]

[15] Shannon, R. T., & Prewitt, C. T. (1969). Effective ionic radii in oxides and fluorides. *Structural Science, 25*(5), 925-946. [CrossRef]

[16] Shi, C., Yan, F., Ge, G., Wei, Y., Zhai, J., & Yao, W. (2021). Significantly enhanced energy storage performances and power density in (1-x)BCZT-xSBT lead-free ceramics via synergistic optimization strategy. *Chemical Engineering Journal, 426*, 130800. [CrossRef]

[17] Zhao, P., Fang, Z., Zhang, X., Chen, J., Shen, Y., Zhang, X., ... & Tang, B. (2021). Aliovalent doping engineering for A-and B-sites with multiple regulatory mechanisms: a strategy to improve energy storage properties of Sr0. 7Bi0. 2TiO3-based lead-free relaxor ferroelectric ceramics. *ACS applied materials & interfaces, 13*(21), 24833-24855. [CrossRef]

Kainat Shah has recently completed her MPhil degree under the supervision of Prof. Raz Muhammad from the Department of Physics, Abdul Wali Khan University Mardan, Pakistan. Her research areas include dielectric materials, multiferroics, and energy storage systems. She has supervised multiple undergraduate research projects in the field of ferroelectric and composite based materials. She is currently engaged in research on hybrid (organic-inorganic) lead-free energy storage materials. (Email: kainat.lfmd@gmail.com)

Asif Ali obtained his MPhil and then enrolled as a PhD scholar in the Department of Physics, Abdul Wali Khan University Mardan, Pakistan. His research focuses on Electroceramics. (Email: asif.lfmd@awkum.edu.pk)